

1 **LIPOSOMAL CO-PERMEATION ASSAY REVEALS**  
2 **UNEXPECTED MEMBRANE INTERACTIONS**  
3 **OF COMMONLY PRESCRIBED DRUGS**

4  
5 Klára Odehnalová<sup>1,‡</sup>, Martin Balouch<sup>1,‡</sup>, Kateřina Storchmannová<sup>2</sup>, Aleš Zadražil<sup>1</sup>,  
6 Karel Berka<sup>2</sup>, František Štěpánek<sup>1,\*</sup>

7  
8 <sup>‡</sup>Both authors contributed equally

9 <sup>1</sup>Department of Chemical Engineering, University of Chemistry and Technology in Prague,  
10 Technická 5, 16628 Prague 6, Czech Republic

11 <sup>2</sup>Department of Physical Chemistry, Faculty of Science, Palacký University Olomouc,  
12 17. listopadu 12, 771 46 Olomouc, Czech Republic

13 \*Corresponding author. E-mail: [stepanef@vscht.cz](mailto:stepanef@vscht.cz); Tel.: +420 220 443 165

14  
15 **ABSTRACT**

16 The permeation of small molecules across biological membranes is a crucial process that lies  
17 at essence of life. Permeation is involved not only in the maintenance of homeostasis at the cell  
18 level but also in the absorption and biodistribution of pharmacologically active substances  
19 throughout the human body. Membranes are formed by phospholipid bilayers that represent an  
20 energy barrier for the permeating molecules. Crossing this energy barrier is assumed to be  
21 a singular event and permeation has traditionally been described as a 1<sup>st</sup> order kinetic process,  
22 proportional only to the concentration gradient of the permeating substance. For a given  
23 membrane composition, permeability was believed to be a unary property dependent only on  
24 the permeating molecule itself. We provide experimental evidence that this long-held view  
25 might not be entirely correct. Liposomes were used in co-permeation experiments with  
26 a fluorescent probe, where simultaneous permeation of two substances occurred over a single  
27 phospholipid bilayer. Using an assay of six commonly prescribed drugs, we have found that the  
28 presence of a co-permeant can either enhance or suppress the permeation rate of the probe  
29 molecule, often more than two-fold in each direction. This can have significant consequences  
30 for the pharmacokinetics and bioavailability of commonly prescribed drugs when used in  
31 combination and provide a new insight into so-far unexplained drug-drug interactions, as well  
32 as changing the perspective on how new drug candidates are evaluated and tested.

33

## 34 INTRODUCTION

35

36 Membrane permeability and water/membrane partitioning coefficient are two key parameters  
37 determining the biodistribution and bioavailability of drugs. They affect the absorption of  
38 a drug upon administration (oral, transdermal, inhalation), its subsequent distribution in the  
39 body and accumulation in individual organs and tissues.

40

41 The rate at which a given molecule permeates across a membrane depends on the energy barrier  
42 represented by the tightly packed phospholipid bilayer. The structure of the lipid bilayer can be  
43 influenced by the presence of other, non-permeating molecules. This phenomenon is called  
44 permeability enhancement and has been studied extensively with regard to skin<sup>19</sup> or intestinal<sup>20</sup>  
45 permeability. Examples of simple permeation enhancers include ethanol, oleic acid, or dimethyl  
46 sulfoxide, but new enhancers and enhancement mechanisms are being actively investigated<sup>21,22</sup>.  
47 An opposite phenomenon – permeation retardation – remains rather unexplored although its  
48 biological and pharmacological implications can be just as important<sup>23</sup>. The ability to suppress  
49 the permeation rate of specific compounds could, for example, enable previously rejected drugs,  
50 which were found to be too “leaky” and thus unsuitable for liposomal formulation<sup>24</sup>, to be  
51 revisited. Not being aware of permeation enhancement or permeation suppression caused by  
52 a medicinal substance that was not *a priori* meant to do so, could be problematic especially in  
53 the context of the so-called polypharmacy patients, who are simultaneously prescribed many  
54 (typically five or more) medicines simultaneously.

55

56 The permeability of a substance across a membrane of given composition has been traditionally  
57 assumed to depend only on the properties of the molecule itself (charge, lipophilicity, molar  
58 weight, etc.). In textbooks, permeation is described as 1<sup>st</sup> order kinetic process, proportional  
59 only to the concentration gradient of the permeating molecule alone. Experimental and  
60 computational permeation results have so far been interpreted in a way that assumed  
61 permeability to be a unary property. However, there is an increasing body of scientific literature  
62 pointing at potential drug-drug interactions in polypharmacy patients, many of whom are  
63 systematically over- or under-dosed due to significantly different bioavailability profiles when  
64 some drugs are prescribed in combination rather than alone<sup>25</sup>. Interestingly, such interactions  
65 were reported even for drugs that target very different metabolic pathways and that should not,

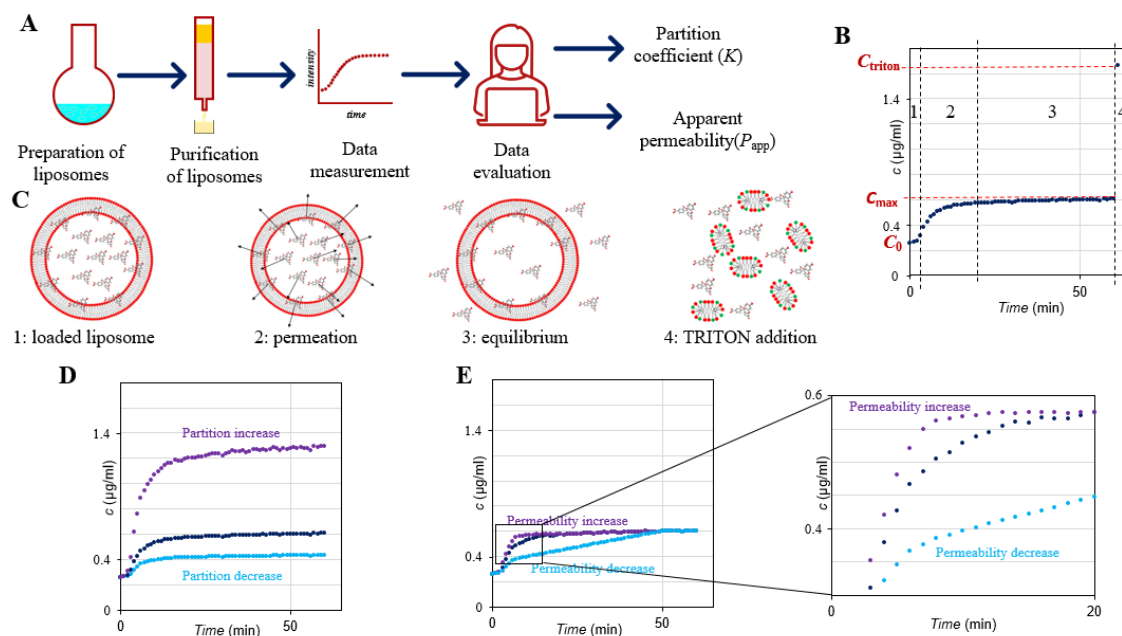
66 in theory, influence each other at the molecular target level. These phenomena could potentially  
67 be explained by considering permeability a binary (or higher order) property, i.e. by considering  
68 that the permeation rate of molecule A could also depend on the concentration of molecule B  
69 (or C, etc.). However, no direct experimental evidence for such collective permeation properties  
70 has been available so far, and in fact there was no method for reliably measuring co-permeation.  
71

72 Experimental methods for studying membrane permeability and partitioning typically rely on  
73 measuring the concentration change of a single permeant in two macroscopic reservoirs  
74 separated by a planar membrane model. The permeation barrier can be formed synthetically  
75 from lipidic materials as in the PAMPA assay<sup>1</sup>, assembled from living cells as in the Caco-2  
76 permeability method<sup>2</sup>, or collected from real tissues such as skin in the Franz diffusion cells<sup>3</sup>.  
77 The interpretation and cross-laboratory comparison of data obtained by the above-mentioned  
78 methods is complicated by the fact that permeation typically occurs across multiple lipid  
79 bilayers, whose exact count is rarely known or reported. Another common feature of the above  
80 methods is that the permeation area is limited to a few square cm, which means that very long  
81 measurement times are needed in the case of low-permeability substances. Therefore,  
82 significant efforts have been devoted also to the development of computational methods for  
83 determining membrane permeability and partitioning of individual molecules<sup>4-7</sup>.

84

85 The problem of low surface area and unknown number of lipid bilayers can be overcome by  
86 replacing the macroscopic planar membrane analogue with liposomes. Liposomes are spherical  
87 molecular assemblies comprising a lipid bilayer enclosing an aqueous core. Their size and  
88 lamellarity can be fairly well controlled<sup>8</sup>. Liposomes are used as drug delivery vehicles thanks  
89 to their proven biocompatibility and tuneable properties. Examples of liposome-based drug  
90 formulations include Doxil®<sup>9</sup>, or recent mRNA COVID-19 vaccines<sup>10,11</sup>. Not all molecules are  
91 directly suitable for liposomal encapsulation<sup>12</sup>. Too high or too low permeability prevents  
92 a drug from being reasonably retained and released from liposomes. Nevertheless, liposomes  
93 lend themselves as a tool for studying permeation and measuring permeability<sup>13</sup>. Methods based  
94 on detecting a pH change induced by the permeation of a weak base into liposomes<sup>14</sup>, on pre-  
95 loading liposomes with engineered receptors whose fluorescence is quenched by the permeating  
96 molecule<sup>15</sup>, or on the so-called immobilized liposome chromatography<sup>16-18</sup> have been reported.  
97

98 Here, we present original co-permeation experimental data obtained by means of a new  
 99 liposome permeation assay on a sample of six commonly prescribed drugs. The principle of the  
 100 method is shown in Fig. 1. Our data reveal both positive and negative interactions of co-  
 101 permeating molecules, providing the first direct evidence of collective permeation and  
 102 partitioning behaviour that could have far-reaching consequences both for the prescription  
 103 practices of existing drugs, and for the evaluation of new ones.  
 104



105  
 106 **Figure 1:** (A) Schematic representation of the liposomal co-permeation method. Liposomes were pre-loaded with  
 107 a fluorescence probe (carboxyfluorescein, CF) and a co-permeant; after separating liposomes from the supernatant,  
 108 the release kinetics into a fresh medium was induced by a temperature step; the release curve was evaluated by  
 109 a mathematical model that provided two parameters: permeability and partitioning coefficient. These were then  
 110 compared between single-component permeation and co-permeation. (B) Typical result of pure CF permeation,  
 111 showing four stages. Stage 1: no release at room temperature; stage 1: permeation after heating to lipid bi-layer  
 112 phase transition; stage 3: equilibrium between intra- and extra-liposomal concentration of the permeant; stage 4:  
 113 dissolution of lipid bilayer by Triton, causing the release of membrane-bound permeant. (C) Schematic  
 114 representation of phenomena that occur during each stage of the experiment. (D) Demonstration of positive and  
 115 negative effect of a co-permeant on the partitioning coefficient (the dark blue symbols represent the original single-  
 116 component permeation). (E) Demonstration of positive and negative effect of a co-permeant on permeability (the  
 117 dark blue symbols represent the original single-component permeation, and the magnified section shows different  
 118 slopes of the release curve).  
 119

## 120 **RESULTS AND DISCUSSION**

121

### 122 **Single-component permeation measurement by liposomal assay**

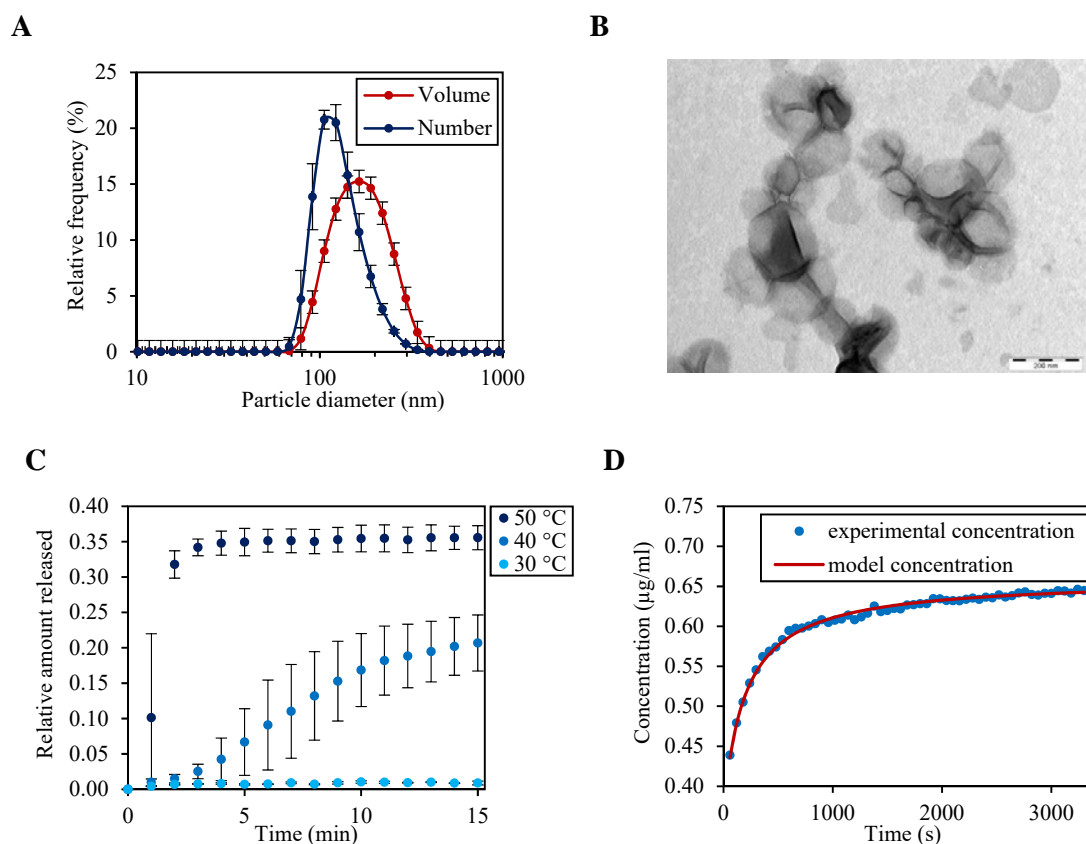
123

124 Dynamic light scattering (Fig. 2A) and TEM (Fig. 2B) analysis of purified liposomes containing  
125 encapsulated carboxyfluorescein (CF) as a fluorescent probe reveals that a population  
126 of liposomes with a mean particle size around 200 nm was prepared. At a lipid concentration  
127 of 5 mg/ml, the total surface area of such liposome is approximately  $2 \text{ m}^2/\text{ml}$ , which represents  
128 an increase by a factor of  $10^4$  compared to traditional permeation assays with planar  
129 membranes. The liposomes were colloidally stable; their zeta potential determined by  
130 electrophoretic light scattering was  $(-12.4 \pm 1.3) \text{ mV}$ . The negative surfaces charge is  
131 consistent with the fact that a negatively charged phospholipid DPPG was used as part of the  
132 membrane mix.

133

134 To utilise liposomes for permeation measurements, the temperature dependence of permeation  
135 rate had to be established first. A lipid bilayer can exist in the gel phase or in the liquid  
136 disordered phase, which differ dramatically in their permeation properties. The phase transition  
137 temperature of the three-component lipid bilayer with cholesterol, which was used in this work,  
138 has been previously shown<sup>26</sup> to be  $41.5 \text{ }^\circ\text{C}$ . In a permeation assay, the liposomes should not be  
139 permeable at laboratory temperature, but it should be possible to start permeation by raising  
140 temperature. Three temperatures were investigated:  $30 \text{ }^\circ\text{C}$ ,  $40 \text{ }^\circ\text{C}$ , and  $50 \text{ }^\circ\text{C}$ . The experiment  
141 was run for 15 minutes. The time dependence of the relative amount of CF released (Fig. 2C)  
142 reveals that at  $30 \text{ }^\circ\text{C}$ , which is safely below the phase transition temperature, there was no  
143 permeation throughout the measurement period. At the other extreme at  $50 \text{ }^\circ\text{C}$ , which is well  
144 above the phase transition temperature, permeation was too rapid, and it would be inaccurate  
145 to evaluate permeability from only a few data points. A suitable temperature thus proved to be  
146  $40 \text{ }^\circ\text{C}$ , which was just below the phase transition but close enough for CF permeation to already  
147 occur at a reasonable rate. The measured CF release curve (time dependence of concentration  
148 over time taken from the inflexion point onwards) was regressed by an algebraic model, detailed  
149 in the Methods section. An excellent agreement between the model and experiment was  
150 obtained (Fig. 2D).

151



152 **Figure 2:** (A) Particle size distribution of liposomes with encapsulated CF, measured by dynamic light scattering.  
 153 (B) TEM micrograph of the prepared liposomes. (C) Thermally induced release of encapsulated CF from  
 154 liposomes at three different temperatures (the phase transition temperature of the used lipid bilayer is 41.5 °C).  
 155 The data points are mean values and error bars indicate standard deviations (n = 3). (D) Comparison of CF release  
 156 curve measured at 40 °C with regression by a mathematical model, which was used for evaluation permeability  
 157 from the experimental data.

158

159 The liposomal permeability of CF in PBS medium had a value of  $(1.4 \pm 0.4) \cdot 10^{-8}$  cm/s, which  
 160 is consistent with previously reported values obtained from the COSMOPerm calculation ( $\approx 10^{-8}$   
 161 cm/s)<sup>4,27</sup>. Furthermore, the partition coefficient was evaluated for this sample according to  
 162 Eq. 3.2, which had a value of  $1.6 \pm 0.1$ . This value is again consistent with COSMOPerm  
 163 calculation ( $\approx 1$ ).

164

### 165 **Direct observation of permeation enhancement mechanisms**

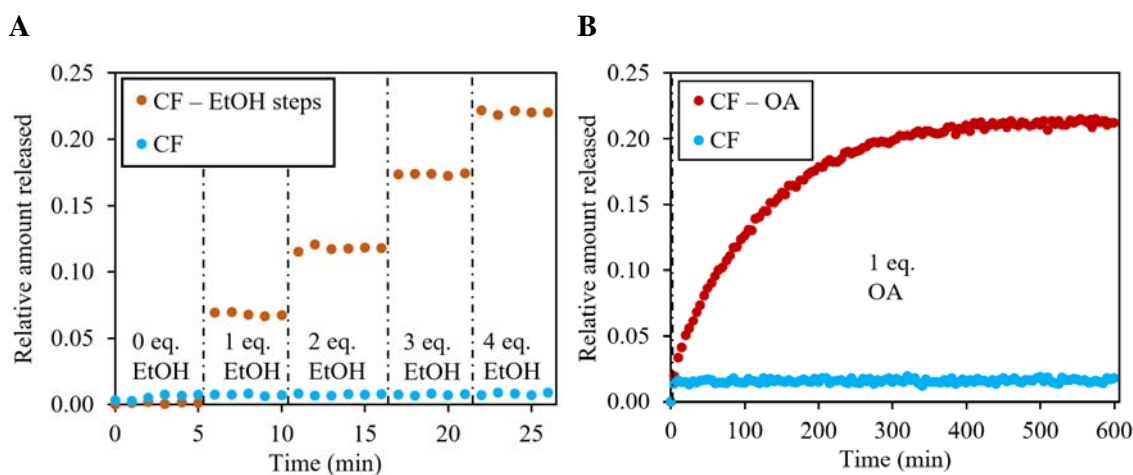
166

167 The liposomal assay employed in this work allows direct observation of permeation  
 168 enhancement in a single layer of phospholipids. Two well-known permeation enhancers with  
 169 different enhancement mechanism were studied: ethanol and oleic acid. Permeation

170 enhancement was investigated at 30 °C, as no CF release occurred at this temperature under  
171 normal conditions. The effect of ethanol was investigated by stepwise addition of small  
172 quantities of ethanol (40 µl in each step) to a spectrophotometric cuvette containing a sample  
173 of liposomes containing CF. A stepwise release of CF from the liposomes was observed  
174 (Fig. 3A) after the addition of each ethanol aliquot. Ethanol is known to cause lipid extraction  
175 from the membrane and to subsequently form a second phase together with the extracted  
176 lipids<sup>28</sup>. After each ethanol addition, release from the affected liposomes was immediate but  
177 other liposomes remained intact as the added ethanol was bound with the extracted lipids. The  
178 increment of CF release in each step corresponds to the liposomes whose membrane integrity  
179 was disrupted by ethanol addition.

180

181 The second studied permeation enhancer was oleic acid. Oleic acid is known to work by a rather  
182 different mechanism than ethanol. Instead of irreversibly damaging liposomes, it incorporates  
183 itself into the membrane structure, slightly disrupts the ordered packing of the phospholipids,  
184 and makes the membrane more permeable to all molecules<sup>29</sup>. Even though the measured  
185 permeation was very slow (CF release occurred over 10 hours), permeability still increased  
186 from a limiting value close to zero to  $6.3 \cdot 10^{-10}$  cm/s (Fig. 3B). The two permeation  
187 enhancement experiments demonstrate the ability of the liposomal assay to capture the effect  
188 of additional chemical species on the permeation rate of the fluorescent probe.



189 **Figure 3:** Experimentally measured dependence of the relative amount of CF released from liposomes on time at  
190 30 °C. (A) Stepwise addition of ethanol into the system. (B) Addition of oleic acid. Note that the duration of the  
191 experiment was 600 min in the case of oleic acid. Blue data points represent the base case (only CF), red data  
192 points represent permeation in the presence of the permeation enhancer.

193

## 194 **Membrane interactions revealed by co-permeation experiments**

195

196 Having established that the liposome permeation assay makes it possible to directly observe  
197 permeation enhancement, we pose the question of whether commonly used pharmaceutical  
198 compounds might inadvertently modulate the membrane permeability and/or partitioning of  
199 another substance. A panel of 6 clinically approved drugs spanning all four Biopharmaceutics  
200 Classification System (BCS) classes<sup>30</sup> has been chosen for co-permeation experiments  
201 (Table 1). Based on their lipophilic/hydrophilic character, the drugs were incorporated into  
202 liposomes either by the aqueous route (i.e., dissolved in the hydration medium together with  
203 CF) or by the lipidic route (i.e., dissolved in chloroform and methanol together with the  
204 membrane lipids). For lipophilic compounds mildly soluble in water (HCTZ and NX), both  
205 loading methods were used (Table 1).

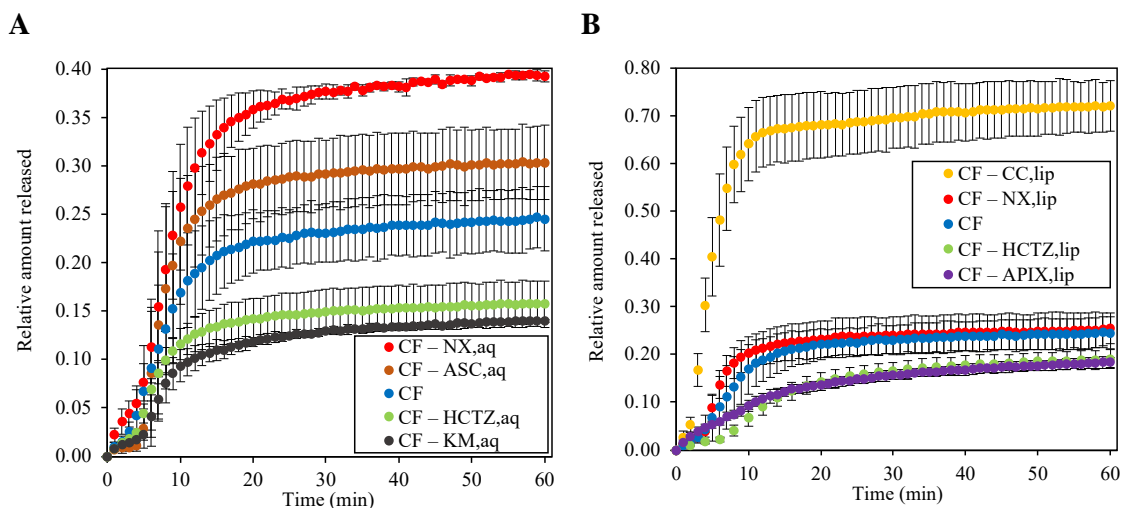
206

207 **Table 1:** Pharmaceutical compounds evaluated in co-permeation experiments, their properties  
208 and concentrations used. Note that CF concentration was 7.5 mg/ml in all cases.

<b>Name and acronym</b>	<b>Indication</b>	<b>BCS Class</b>	<b>Properties</b>	<b>Liposome incorporation route and concentration</b>
Ascorbic acid (ACS)	Essential vitamin	Class I	well soluble well permeable	aqueous (15 mg/ml)
Hydrochlorothiazide (HCTZ)	Hypertension	Class II	mildly soluble (0.72 mg/ml <sup>31</sup> ) well permeable	lipidic & aqueous (0.5 mg/ml)
Kanamycin (KM)	Antibiotic	Class III	well soluble poorly permeable	aqueous (15 mg/ml)
Norfloxacin (NX)	Antibiotic	Class IV	mildly soluble (0.28 mg/ml <sup>32</sup> ) poorly permeable	lipidic & aqueous (0.2 mg/ml)
Candesartan cilexetil (CC)	Hypertension	Class II	poorly soluble well permeable	lipidic (0.5 mg/ml)
Apixaban (APIX)	Anticoagulant	Class IV	poorly soluble poorly permeable	lipidic (0.5 mg/ml)

209





210 **Figure 4:** Relative amount of CF released as function time in binary co-permeation experiments conducted using  
 211 liposomal assay at 40 °C. (A) Substances incorporated into liposomes by the aqueous route. (B) Substances  
 212 incorporated into liposomes by the lipidic route. The permeation of CF alone is shown in both cases for reference.  
 213 The acronyms of individual substances are given in Table 1. The data points are mean values, the error bars  
 214 represent standard deviations (n = 3). Note the difference in the y-axis scale between cases (A) and (B).

215

216 Unexpected phenomena were observed during binary co-permeation experiments (Fig. 4). All  
 217 investigated pharmaceutical substances (regardless of their molar weight, aqueous solubility,  
 218 lipophilicity or BCS class) had a manifestable and sometimes very strong effect on CF  
 219 permeation, although these substances are not *a priori* meant to act as permeation enhancers or  
 220 retardants, and no such behaviour has been reported for them before. An increase in the  
 221 asymptotic quantity released of CF was found for binary co-permeation with ASC<sub>aq</sub>, NX<sub>aq</sub>, and  
 222 CC<sub>lip</sub>, whereas a decrease was found for HCTZ<sub>aq</sub>, KM<sub>aq</sub>, HCTZ<sub>lip</sub>, and APIX<sub>lip</sub> (Fig. 4).  
 223 Curiously, the increase in the relative amount released was caused by a pair of substances from  
 224 exactly opposite BCS classes: ASC with high solubility and high permeability and NX with  
 225 low solubility and low permeability. The same was true for the two substances that reduced the  
 226 relative amount released: HCTZ with a low solubility and high permeability and KM with  
 227 a high solubility and low permeability. These results suggest that solubility/permeability of the  
 228 co-permeating substance alone is insufficient to determine its effect on the quantity released of  
 229 the fluorescent probe. Clearly, both antagonistic and synergistic effects between the permeants  
 230 exist, and these are sufficiently strong to change CF membrane partitioning 2-5x in both  
 231 directions, and permeability up to 2x upwards and up to 6x downwards (Table 2). From the  
 232 point of view of pharmacokinetics, such changes due to drug-membrane interaction could have  
 233 dramatic therapeutic implications and could potentially lead to incorrect prescription and dosing

234 decisions, which are typically made on the assumption that each drug behaves as if it were in  
235 the patient's body alone. As no simple rule based on the BCS class can explain the experimental  
236 data, let us briefly consider the specific features of each permeant.

237

238 **Table 2:** Experimentally determined values of permeability and partition coefficient for CF  
239 alone and in co-permeation in binary mixtures with selected drugs added to the liposomal assay  
240 either by the aqueous or lipidic route.

Sample	Permeability (cm/s)	Partition coefficient
CF alone	$(1.4 \pm 0.4) \cdot 10^{-8}$	$1.6 \pm 0.1$
CF-ASC <sub>aq</sub>	$(2.4 \pm 0.7) \cdot 10^{-8}$	$1.4 \pm 0.2$
CF-HCTZ <sub>aq</sub>	$(1.5 \pm 0.3) \cdot 10^{-8}$	$3.5 \pm 0.5$
CF-KM <sub>aq</sub>	$(1.2 \pm 0.3) \cdot 10^{-8}$	$3.9 \pm 0.1$
CF-NX <sub>aq</sub>	$(2.3 \pm 0.5) \cdot 10^{-8}$	$0.92 \pm 0.04$
CF-CC <sub>lip</sub>	$(2.2 \pm 0.7) \cdot 10^{-8}$	$0.32 \pm 0.09$
CF-APIX <sub>lip</sub>	$(3.1 \pm 0.4) \cdot 10^{-9}$	$1.9 \pm 0.1$
CF-HCTZ <sub>lip</sub>	$(1.1 \pm 0.1) \cdot 10^{-8}$	$2.7 \pm 0.3$
CF-NX <sub>lip</sub>	$(2.2 \pm 0.2) \cdot 10^{-8}$	$2.1 \pm 0.3$

241

242 **Ascorbic acid** (ASC) was added only by the aqueous route and caused CF permeability to be  
243 approximately doubled while the partition coefficient remained the same within the  
244 measurement error. Ascorbic acid is predominantly present in the anionic form (Table 3).  
245 Therefore, we suggest that this permeability increase can be influenced by the molecule charge.  
246 The negatively charged ASC molecules can locally increase the distances between the polar  
247 heads of the lipid molecules and therefore increase the permeation rate of CF through the  
248 membrane without affecting its partitioning coefficient. Thus, co-permeation with ASC has an  
249 enhancing effect on CF permeation.

250

251 **Hydrochlorothiazide** (HCTZ) and **Kanamycin** (KM) had the same effect on the permeation  
252 properties of CF (permeability remained the same within the measurement error, but the  
253 partition coefficient increased). Therefore, a similarity was sought between these substances.  
254 Both KM and HCTZ have ionizable NH<sub>2</sub> groups (Table 3), which allows both molecules to  
255 exist in a slightly positively charged form at the experimental pH 7.4. Either a change in the

256 membrane packing, or a temporary association with CF, could cause an increase of membrane  
257 partitioning. It should be noted that the increase in CF partitioning coefficient is different for  
258 HCTZ samples made by the aqueous and the lipid route (Table 2). This could be caused by the  
259 different amount of HCTZ remaining in the sample after liposome purification.

260

261 **Norfloxacin** (NX) again nearly doubled CF permeability, but the change of CF partition  
262 coefficient depends on the method of addition. At pH 7.4, NX is primarily a zwitterion, but  
263 since both the basic and acidic pKa is close to the used pH (7.4), there is a non-negligible  
264 amount of both anionic and cationic form. An approximate ratio of the three forms is  
265 zwitterion : anion : cation = 89 : 7 : 4. The anion can play the same role in increasing CF  
266 permeability as in the case of ASC described above. The difference in the partition coefficient  
267 for both ways of addition remains unclear.

268

269 **Candesartan cilexetil** (CC) occurs in a slightly negatively charged form, and the trend for  
270 enhancing CF permeability was confirmed, similarly to ASC and NX. Furthermore, there was  
271 a significant decrease in the partition coefficient. This may have been because CC is a very  
272 lipophilic and large molecule, which may have displaced CF from the membrane by its presence  
273 in the membrane during co-permeation. Consequently, the partition coefficient of CF was  
274 significantly reduced.

275

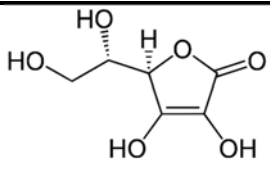
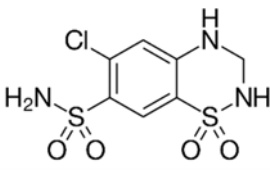
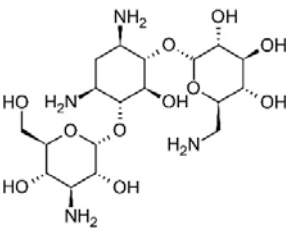
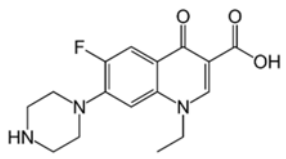
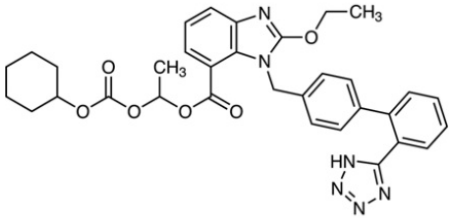
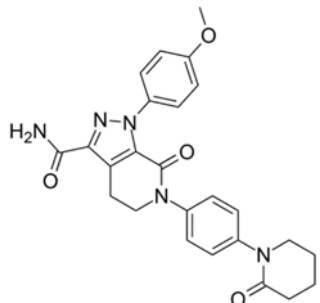
276 **Apixaban** (APIX) caused an approximately sixfold decrease in permeability for CF. This could  
277 be because APIX is an uncharged rigid molecule that may very distantly resemble sterols.  
278 Theoretically, it could incorporate into the membrane during co-permeation, increasing its  
279 rigidity and decrease its permeability for CF. Further correlative evidence for this hypothesis is  
280 the plot of the relative amount released. When CF is mixed with this substance, the curve has  
281 no inflexion point, as is the case for all mixtures with other substances. At the same time,  
282 however, its incorporation does not seem to affect the partition coefficient in any way, so its  
283 presence does not displace CF from the membrane.

284

285 A detailed mechanistic explanation of how each of the investigated substances might affect CF  
286 permeability and partitioning coefficient will be obtained by molecular dynamics simulations,  
287 but this is beyond the scope of the present Communication.

288

289 **Table 3:** Properties of substances used during co-permeation experiments with CF.

Substance	Molecule structure	pKa	Charge at pH 7.4
ASC		acidic 4.7	negative
HCTZ		basic 7.9	slightly positive
KM		basic 9.5	positive
NX		acidic 6.3 basic 8.8	prevalently zwitterion
CC		acidic 6.0	slightly negative
APIX		—	neutral

290

## 291 **CONCLUSION**

292

293 Using a novel permeation measurement methodology based on a liposomal assay, the  
294 permeation enhancement or suppression during co-permeation of two substances has been  
295 directly investigated for the first time. As a methodology validation after the selection of an  
296 appropriate temperature, two agents with known permeation enhancement properties due to  
297 membrane disruption were studied (ethanol and oleic acid). In the case of ethanol addition,  
298 a stepwise release of the permeant (CF) was observed. This was due to the extraction of lipids  
299 from the membrane by ethanol and the loss of membrane integrity in the affected the liposomes  
300 from which CF could leak out. Oleic acid worked on a different principle, which, due to its  
301 incorporation into the membrane, caused gradual permeation of CF even at 30 °C, i.e., well  
302 below the phase transition of the original membrane. A mathematical model of permeation  
303 enables the quantitative evaluation of permeability and the membrane partitioning coefficient  
304 of the permeant.

305

306 The liposomal permeation assay was then used for investigating the effect of six commonly  
307 prescribed pharmaceutical substances on permeability and partition coefficient during binary  
308 co-permeation experiments. The chosen substances are not meant to act as permeation  
309 modifiers and no such behaviour has been measured or reported for these molecules before.  
310 Unexpectedly, all six investigated substances were found to have a significant effect on the  
311 permeability and/or partitioning coefficient of the permeant. Depending on the substance, either  
312 enhancement or suppression of permeation was observed (by a factor of up to 6x). The  
313 membrane partitioning coefficient was influenced by a factor of up to 5x, again both upwards  
314 and downwards depending on the co-permeant. There was no simple correlation between the  
315 BCS class of the investigated drug and its effect on permeation. Specific molecular interactions  
316 with the permeant (CF) and/the membrane lipids were therefore likely the cause of permeation  
317 modification in each case.

318

319 The liposomal co-permeation assay introduced in this Communication is fast and reproducible.  
320 The results indicate unexpected and previously unknown drug-membrane interactions that can  
321 have far-reaching consequences for the pharmacokinetics of commonly prescribed drugs in  
322 polypharmacy patients. As both permeability and the membrane partitioning coefficient can be  
323 upregulated or downregulated several times in a manner that is difficult to predict simply from

324 the molecular properties, this work highlights the need for a systematic screening of currently  
325 prescribed drugs for interactions at the permeation and biodistribution level, rather than at the  
326 metabolic level. The knowledge obtained in such co-permeation screening should then lead to  
327 better informed prescription and dosage decisions by physicians who so-far rely solely on  
328 single-molecule data.

329

## 330 **METHODS**

331

### 332 **Materials**

333 Phosphate-buffered saline in tablets (PBS), 5(6)-carboxyfluorescein (CF, >95%), norfloxacin  
334 (NX, >98%), cholesterol (>99%), kanamycin sulfate (KM), TRITON X-100®  
335 (laboratory grade), and oleic acid (OA, 90%) were purchased from Sigma-Aldrich s.r.o.  
336 Dipalmitoylphosphoglycerole (DPPG) and dipalmitoylphosphatidylcholine (DPPC) were  
337 purchased from Corden Pharma. Sodium hydroxide (NaOH, p. a.), ascorbic acid (ASC, p. a.),  
338 sodium chloride (NaCl, p. a.) phosphoric acid (H<sub>3</sub>PO<sub>4</sub>, >75%), and disodium hydrogen  
339 phosphate dodecahydrate (Na<sub>2</sub>HPO<sub>4</sub> · 12 H<sub>2</sub>O) were purchased from PENTA s.r.o. Chloroform  
340 (p. a.), and ethanol (EtOH, >99.8%) were purchased from Lach-Ner s.r.o. and methanol  
341 (>99.8%) was purchased from Fisher Scientific s.r.o. Hydrochlorothiazide (HCTZ),  
342 candesartan cilexetil (CC) and apixaban (APIX) were kindly provided by Zentiva k.s. All  
343 substances and materials were used as supplied and were not modified. Deionized water (Aqual  
344 25, 0.07 μS/cm) was used in all experiments.

345

### 346 **Preparation of liposomes**

347 Liposomes were prepared by the standard lipid film hydration method. the mixture of  
348 phospholipids and cholesterol (8.1 mg DPPC, 1.1 mg DPPG, 0.9 mg cholesterol) was dissolved  
349 in 10 ml of methanol:chloroform solution (1:1 by volume). Subsequently, the solvent mixture  
350 was evaporated on a vacuum rotary evaporator (60 °C, gradually reducing the pressure from  
351 atmospheric to approximately 80 mbar). This process produced a dried lipid film which was  
352 subsequently dried in a desiccator for at least 3 hours (30 mbar).

353 The completely dried lipid film was then hydrated with 2 ml of aqueous medium  
354 (7.5 mg/ml of carboxyfluorescein solution in PBS, pH 7.4). The sample and the extruder  
355 (Avanti Mini Extruder) were heated to 69 °C for 10 minutes and the sample was then vortexed

356 to form polydisperse multilamellar liposomes. To increase the uniformity, the sample was  
357 extruded at least 21 times through a membrane with a pore size of 200 nm (at 69 °C).

358 The prepared liposomes were characterized. Particle size distribution was determined  
359 using dynamic light scattering (DLS), the zeta potential was determined using electrophoretic  
360 light scattering (ELS) (both Malvern Zeta sizer Nano-ZS), and by images from a transmission  
361 electron microscope (TEM – Jeol JEM-1010 – accelerating voltage 80 kV).

362

### 363 **Encapsulation of co-permeants**

364 The hydrophilic substances (ascorbic acid and kanamycin) and the mildly soluble lipophilic  
365 substances (hydrochlorothiazide and norfloxacin) were added to the hydration medium  
366 (solution CF in PBS) during lipid film hydration (aqueous addition route). Lipophilic  
367 substances (apixaban, candesartan cilexetil, hydrochlorothiazide and norfloxacin) were added  
368 during the first step of liposome preparation, i.e., they were mixed with the phospholipids and  
369 dissolved in a mixture of chloroform and methanol (lipid addition route). All samples were  
370 prepared in triplicates.

371

### 372 **Purification of liposomes**

373 All liposome samples were purified by size exclusion chromatography using PD Minitrap™ G-  
374 25 separation columns to separate the surrounding hydration solution from the liposomes  
375 themselves. In this way, 1 ml of purified liposome solution was collected. The principle of CF  
376 release kinetics measurement is based on the fluorescence quenching of concentrated CF. The  
377 intraliposomal CF does not fluoresce; its fluorescence increases sharply only upon dilution after  
378 release from the liposomes. For this reason, the hydration medium had to be separated from the  
379 liposomes before conducting any permeation experiments.

380

### 381 **Permeation measurement**

382 From a stock of purified liposomes, 60 µl was pipetted into a disposable cuvette and mixed with  
383 1140 µl of PBS. Then the measurement (in triplicates for each sample) of CF permeation  
384 through the membrane was carried out in a fluorescence spectrophotometer (Cary Eclipse,  
385 Agilent) in which the sample was heated to the desired temperature (30 °C, 40 °C and 50 °C),  
386 which was kept constant throughout the measurement. The following settings were used:  
387 excitation wavelength 490 nm, emission wavelength 522 nm, excitation slit: 2.5 and 2.5, scan  
388 control: slow, detector voltage: medium, maximum intensity: 1000 a.u.. The time dependence

389 of the fluorescence intensity at constant temperatures was measured. At the end of the  
390 experiment, 5  $\mu\text{l}$  of ten times diluted TRITON X-100<sup>®</sup> was added to cause total micellization  
391 of the system, thus releasing all previously unreleased CF. The mechanism of this micellization  
392 is shown in Fig. 1C and is based on molecular dynamics study<sup>33</sup>. The measured fluorescence  
393 intensity dependence on time was then converted to CF concentration using a calibration curve.  
394 The relative amount released of CF was then determined:

$$395 \quad \text{Relative amount released} = \frac{c_{t,\text{CF}} - c_{1,\text{CF}}}{c_{\text{triton,CF}} - c_{1,\text{CF}}}, \quad (1)$$

396 where  $c_{t,\text{CF}}$  is the mass concentration of CF at a time  $t$ ,  $c_{1,\text{CF}}$  is the CF mass concentration  
397 at the beginning of the measurement, and  $c_{\text{triton,CF}}$  is the final CF mass concentration after  
398 liposome micellization by the addition of TRITON X-100<sup>®</sup>. The partition coefficient was  
399 calculated from the mass balance using the relation:

$$400 \quad K_{\text{CF}} = \frac{c_{\text{triton,CF}} - c_{\text{fin,CF}}}{c_{\text{fin,CF}}}, \quad (2)$$

401 where  $c_{\text{fin,CF}}$  is the asymptotic mass concentration of CF achieved by thermal release, i.e. the  
402 final concentration at the end of the experiment just before TRITON addition.

403

#### 404 **Permeation enhancers**

405 For the study of permeation enhancers, CF-containing liposomes were prepared and purified as  
406 described above. For permeation enhancement by ethanol, 60  $\mu\text{l}$  of purified liposomes with  
407 encapsulated CF was mixed with 1140  $\mu\text{l}$  of PBS in a measuring cuvette. The samples were  
408 maintained at 30 °C. At approximately 5-minutes intervals, 40  $\mu\text{l}$  of ethanol was added  
409 to the measuring cuvette from the top and the fluorescence intensity was measured by  
410 fluorescence spectrophotometry as described above. For permeation enhancement by oleic acid,  
411 the procedure was very similar to ethanol, only the volumes were different (50  $\mu\text{l}$  oleic acid,  
412 1090  $\mu\text{l}$  PBS) and only one addition at the start of the experiment was done. The temperature  
413 was also 30 °C.

414

#### 415 **Model for permeability determination**

416 The model was used for evaluating permeability from its definition, using the dependence of  
417 concentration on time:

$$418 \quad j_{\text{CF}} = P_{\text{erm,CF}} \cdot (c_{\text{liposome,CF}} - c_{t,\text{CF}}), \quad (3)$$

419 where  $j_{\text{CF}}$  is a flux of the permeating substance,  $P_{\text{erm,CF}}$  is its permeability, and  $c_{\text{liposome,CF}}$  is the  
420 mass concentration of CF inside the liposomes. The previously mentioned  $c_{t,\text{CF}}$  was calculated



421 using the calibration curve from the measured fluorescence intensity over time. The unknown  
 422 quantity  $c_{\text{liposome,CF}}$ , was obtained from the mass balance, considering that the total quantity of  
 423 CF, which is known, is present in the liposomal lumen, in the membrane, in the bulk outside  
 424 liposomes. We start with the basic expression:

$$425 \quad c_{\text{liposome,CF}} = \frac{m_{\text{liposome,CF}}}{V_{\text{liposome}}}, \quad (4)$$

426 where  $m_{\text{liposome,CF}}$  is the mass of CF inside the liposomes and  $V_{\text{liposome}}$  is the volume inside  
 427 the liposomes in the measured sample, and combine it with the mass balance:

$$428 \quad m_{\text{liposome,CF}} = m_{\text{total,CF}} - m_{\text{lipids,CF}} - m_{\text{t,CF}}, \quad (5)$$

429 where  $m_{\text{total,CF}}$  is the total encapsulated mass of CF in the sample,  $m_{\text{t,CF}}$  is the measured mass  
 430 of CF in bulk outside liposomes at time  $t$ , and  $m_{\text{lipids,CF}}$  is the mass of CF in the membrane,  
 431 which is released only after TRITON addition and is expressed as:

$$432 \quad m_{\text{lipids,CF}} = m_{\text{total,CF}} - m_{\text{fin,CF}}. \quad (6)$$

433 Using this equation, eq. (3.5) becomes:

$$434 \quad m_{\text{liposome,CF}} = m_{\text{fin,CF}} - m_{\text{t,CF}}, \quad (7)$$

435 where  $m_{\text{fin,CF}}$  is the final mass of CF released during the experiment only by diffusion (i.e.  
 436 before TRITON addition). For the determination of  $m_{\text{fin,CF}}$  and  $m_{\text{t,CF}}$  it was necessary to use the  
 437 conversion using the volume of the diluted sample (volume in the cuvette,  $V_{\text{cuvette}}$ ) and a certain  
 438 concentration ( $c_{\text{j,CF}}$ ), which was evaluated from the measured intensity using a calibration  
 439 curve:

$$440 \quad m_{\text{j,CF}} = c_{\text{j,CF}} \cdot V_{\text{cuvette}} \quad (8)$$

441 Next, it was necessary to express  $V_{\text{liposome}}$  in (eq. 3.4) as follows:

$$442 \quad V_{\text{liposome}} = V_{\text{liposome,1}} \cdot N_{\text{liposome}}, \quad (9)$$

443 where  $V_{\text{liposome,1}}$  is the volume inside one liposome and  $N_{\text{liposome}}$  is the number of liposomes  
 444 in the measured sample.  $V_{\text{liposome,1}}$  could be determined with the following equation:

$$445 \quad V_{\text{liposome,1}} = \frac{\pi}{6} \cdot d_{\text{liposome,in}}^3, \quad (10)$$

446 where  $d_{\text{liposome,in}}$  is the inner diameter of the liposomes and was determined as follows:

$$447 \quad d_{\text{liposome,in}} = d_{\text{liposome,volume}} - 2 \cdot d_{\text{membrane}}, \quad (11)$$

448 where  $d_{\text{liposome,volume}}$  is the volume-weighted diameter measured by dynamic light scattering  
 449 (Malvern Zetasizer) and  $d_{\text{membrane}}$  is 4.059 nm<sup>34</sup> for using the composition. In eq. 9,  $N_{\text{liposome}}$   
 450 was also expressed as:

451 
$$N_{\text{liposome}} = \frac{m_{\text{lipid,sample}}}{m_{\text{lipid,1liposome}}}, \quad (12)$$

452 where  $m_{\text{lipid,sample}}$  is the mass of lipids in the measured sample and  $m_{\text{lipid,1liposome}}$  is the mass  
 453 of lipids that form one liposome. The first mentioned was further modified to:

454 
$$m_{\text{lipid,sample}} = c_{\text{lipid,sample}} \cdot V_{\text{sample}}, \quad (13)$$

455 where  $V_{\text{sample}}$  is the volume of the concentrated liposome sample, which is further diluted  
 456 to the volume  $V_{\text{cuvette}}$  and measured. Furthermore,  $c_{\text{lipid,sample}}$  (which is the mass concentration  
 457 of lipids in this sample volume –  $V_{\text{sample}}$ ) was determined as follows:

458 
$$c_{\text{lipid,sample}} = \frac{m_{\text{lipid,column}}}{V_{\text{lipid,column}}}, \quad (14)$$

459 where  $m_{\text{lipid,column}}$  is the mass of lipids to be purified on the column, which was 5 mg for all  
 460 experiments and  $V_{\text{lipid,column}}$  is the volume of the sample taken from the column, which was  
 461 1 ml for all experiments. From eq. 12,  $m_{\text{lipid,1liposome}}$  was also modified:

462 
$$m_{\text{lipid,1liposome}} = n_{\text{lipid,1liposome}} \cdot M_{\text{lipid}}, \quad (15)$$

463 where  $n_{\text{lipid,1liposome}}$  is the molar amount of lipids that form a single liposome and  $M_{\text{lipid}}$  is  
 464 the mean molar mass of the lipids used (DPPC, DPPG, Cholesterol):

465 
$$M_{\text{lipid}} = \sum(x_{\text{lipid,l}} \cdot M_{\text{lipid,l}}), \quad (16)$$

466 where  $x_{\text{lipid,l}}$  is the molar fraction of lipid  $l$  and  $M_{\text{lipid,l}}$  is the molar mass of the lipid  $l$ .  
 467 For the composition used and the molar ratio of lipids was  $M_{\text{lipid}} = 683.02$  g/mol. From eq. 15,  
 468  $n_{\text{lipid,1liposome}}$  was determined by definition:

469 
$$n_{\text{lipid,1liposome}} = \frac{N_{\text{lipid,1liposome}}}{N_A}, \quad (17)$$

470 where  $N_A$  is Avogadro's number and  $N_{\text{lipid,1liposome}}$  is the number of lipids that form a single  
 471 liposome, and it was determined as follows:

472 
$$N_{\text{lipid,1liposome}} = \frac{2 \cdot A_{\text{liposome,1}}}{A_{\text{lipid,1}}}, \quad (18)$$

473 where  $A_{\text{lipid,1}}$  is the area of one lipid, which is  $47.9 \text{ \AA}^2$ <sup>35</sup>. Since the liposome is made up  
 474 of a lipid bilayer, it should be considered that the liposome has a double area (inner and outer).  
 475 Therefore, the area of the liposome is multiplied by two.  $A_{\text{liposome,1}}$  is the surface of one  
 476 liposome through which the substance  $i$  permeates:

477 
$$A_{\text{liposome,1}} = \pi \cdot \left( \frac{d_{\text{liposome,volume}} + d_{\text{liposome,in}}}{2} \right)^2 \quad (19)$$

478 The left side of eq. 3 has also been modified as follows:

479 
$$j_{CF} = \frac{\dot{m}_{\text{through,CF}}}{A_{\text{liposome,total}}} = \frac{m_{\text{through,CF}}}{A_{\text{liposome,total}} \cdot t}, \quad (20)$$

480 where  $\dot{m}_{\text{through,CF}}$  is the mass flow of CF passing through the liposomal membrane,  $A_{\text{liposome,total}}$   
481 is the total surface of all liposomes in the measured sample,  $t$  is time, and  $m_{\text{through,CF}}$  is the mass  
482 of CF passing through the liposomal membrane:

483 
$$m_{\text{through,CF}} = m_{t,\text{CF}} - m_{1,\text{CF}}, \quad (21)$$

484 where  $m_{1,\text{CF}}$  is the initial mass of CF in the area around the liposomes before release and was  
485 determined by eq. 8.  $A_{\text{liposome,total}}$  was determined as follows:

486 
$$A_{\text{liposome,total}} = A_{\text{liposome,1}} \cdot N_{\text{liposome}}, \quad (22)$$

487 where  $A_{\text{liposome,1}}$  was determined from eq. 19 and  $N_{\text{liposome}}$  from eq. 12.

488

489 **REFERENCES**

- 490 1. Kansy, M.; Senner, F.; Gubernator, K., Physicochemical High Throughput Screening:  
491 Parallel Artificial Membrane Permeation Assay in the Description of Passive Absorption  
492 Processes. *Journal of Medicinal Chemistry* **1998**, *41* (7), 1007-1010.
- 493 2. Hidalgo, I. J.; Raub, T. J.; Borchardt, R. T., Characterization of the human colon  
494 carcinoma cell line (Caco-2) as a model system for intestinal epithelial permeability.  
495 *Gastroenterology* **1989**, *96* (3), 736-749.
- 496 3. Vovesná, A.; Zhigunov, A.; Balouch, M.; Zbytovská, J., Ceramide liposomes for skin  
497 barrier recovery: A novel formulation based on natural skin lipids. *International Journal of*  
498 *Pharmaceutics* **2021**, *596*, 120264.
- 499 4. Schwöbel, J. A. H.; Ebert, A.; Bittermann, K.; Huniar, U.; Goss, K.-U.; Klamt, A.,  
500 COSMOperm: Mechanistic Prediction of Passive Membrane Permeability for Neutral  
501 Compounds and Ions and Its pH Dependence. *The Journal of Physical Chemistry B* **2020**, *124*  
502 (16), 3343-3354.
- 503 5. Lomize, A. L.; Pogozheva, I. D., Physics-Based Method for Modeling Passive  
504 Membrane Permeability and Translocation Pathways of Bioactive Molecules. *Journal of*  
505 *Chemical Information and Modeling* **2019**, *59* (7), 3198-3213.
- 506 6. Fujikawa, M.; Ano, R.; Nakao, K.; Shimizu, R.; Akamatsu, M., Relationships between  
507 structure and high-throughput screening permeability of diverse drugs with artificial  
508 membranes: Application to prediction of Caco-2 cell permeability. *Bioorganic & Medicinal*  
509 *Chemistry* **2005**, *13* (15), 4721-4732.
- 510 7. Lee, C. T.; Comer, J.; Herndon, C.; Leung, N.; Pavlova, A.; Swift, R. V.; Tung, C.;  
511 Rowley, C. N.; Amaro, R. E.; Chipot, C.; Wang, Y.; Gumbart, J. C., Simulation-Based  
512 Approaches for Determining Membrane Permeability of Small Compounds. *Journal of*  
513 *Chemical Information and Modeling* **2016**, *56* (4), 721-733.
- 514 8. Has, C.; Sunthar, P., A comprehensive review on recent preparation techniques of  
515 liposomes. *Journal of Liposome Research* **2020**, *30* (4), 336-365.
- 516 9. Barenholz, Y., Doxil® — The first FDA-approved nano-drug: Lessons learned. *Journal*  
517 *of Controlled Release* **2012**, *160* (2), 117-134.
- 518 10. Jackson, L. A.; Anderson, E. J.; Roupheal, N. G.; Roberts, P. C.; Makhene, M.; Coler,  
519 R. N.; McCullough, M. P.; Chappell, J. D.; Denison, M. R.; Stevens, L. J.; Pruijssers, A. J.;  
520 McDermott, A.; Flach, B.; Doria-Rose, N. A.; Corbett, K. S.; Morabito, K. M.; O'Dell, S.;  
521 Schmidt, S. D.; Swanson, P. A.; Padilla, M.; Mascola, J. R.; Neuzil, K. M.; Bennett, H.;

- 522 Sun, W.; Peters, E.; Makowski, M.; Albert, J.; Cross, K.; Buchanan, W.; Pikaart-Tautges,  
523 R.; Ledgerwood, J. E.; Graham, B. S.; Beigel, J. H., An mRNA Vaccine against SARS-CoV-  
524 2 — Preliminary Report. *New England Journal of Medicine* **2020**, *383* (20), 1920-1931.
- 525 11. Mulligan, M. J.; Lyke, K. E.; Kitchin, N.; Absalon, J.; Gurtman, A.; Lockhart, S.;  
526 Neuzil, K.; Raabe, V.; Bailey, R.; Swanson, K. A.; Li, P.; Koury, K.; Kalina, W.; Cooper,  
527 D.; Fontes-Garfias, C.; Shi, P.-Y.; Türeci, Ö.; Tompkins, K. R.; Walsh, E. E.; Frenck, R.;  
528 Falsey, A. R.; Dormitzer, P. R.; Gruber, W. C.; Şahin, U.; Jansen, K. U., Phase I/II study of  
529 COVID-19 RNA vaccine BNT162b1 in adults. *Nature* **2020**, *586* (7830), 589-593.
- 530 12. Crommelin, D. J. A.; van Hoogevest, P.; Storm, G., The role of liposomes in clinical  
531 nanomedicine development. What now? Now what? *Journal of Controlled Release* **2020**, *318*,  
532 256-263.
- 533 13. Nasr, G.; Greige-Gerges, H.; Elaissari, A.; Khreich, N., Liposomal membrane  
534 permeability assessment by fluorescence techniques: Main permeabilizing agents, applications  
535 and challenges. *International Journal of Pharmaceutics* **2020**, *580*, 119198.
- 536 14. Eyer, K.; Paech, F.; Schuler, F.; Kuhn, P.; Kissner, R.; Belli, S.; Dittrich, P. S.;  
537 Krämer, S. D., A liposomal fluorescence assay to study permeation kinetics of drug-like weak  
538 bases across the lipid bilayer. *Journal of Controlled Release* **2014**, *173*, 102-109.
- 539 15. Biedermann, F.; Ghale, G.; Hennig, A.; Nau, W. M., Fluorescent artificial receptor-  
540 based membrane assay (FARMA) for spatiotemporally resolved monitoring of biomembrane  
541 permeability. *Communications Biology* **2020**, *3* (1), 383.
- 542 16. Li, H.; Zhao, T.; Sun, Z., Analytical techniques and methods for study of drug-lipid  
543 membrane interactions. *Reviews in Analytical Chemistry* **2018**, *37* (1).
- 544 17. Liu, G.; Hou, S.; Tong, P.; Li, J., Liposomes: Preparation, Characteristics, and  
545 Application Strategies in Analytical Chemistry. *Critical Reviews in Analytical Chemistry* **2022**,  
546 *52* (2), 392-412.
- 547 18. Österberg, T.; Svensson, M.; Lundahl, P., Chromatographic retention of drug molecules  
548 on immobilised liposomes prepared from egg phospholipids and from chemically pure  
549 phospholipids. *European Journal of Pharmaceutical Sciences* **2001**, *12* (4), 427-439.
- 550 19. Hadgraft, J.; Lane, M. E., Skin permeation: The years of enlightenment. *International*  
551 *Journal of Pharmaceutics* **2005**, *305* (1), 2-12.
- 552 20. Aungst, B. J., Intestinal Permeation Enhancers. *Journal of Pharmaceutical Sciences*  
553 **2000**, *89* (4), 429-442.

- 554 21. Gupta, R.; Badhe, Y.; Rai, B.; Mitragotri, S., Molecular mechanism of the skin  
555 permeation enhancing effect of ethanol: a molecular dynamics study. *RSC Advances* **2020**, *10*  
556 (21), 12234-12248.
- 557 22. Lundborg, M.; Wennberg, C. L.; Narangifard, A.; Lindahl, E.; Norlén, L., Predicting  
558 drug permeability through skin using molecular dynamics simulation. *Journal of Controlled*  
559 *Release* **2018**, *283*, 269-279.
- 560 23. Kaushik, D.; Batheja, P.; Kilfoyle, B.; Rai, V.; Michniak-Kohn, B., Percutaneous  
561 permeation modifiers: enhancement versus retardation. *Expert Opinion on Drug Delivery* **2008**,  
562 *5* (5), 517-529.
- 563 24. Balouch, M.; Storchmannová, K.; Štěpánek, F.; Berka, K., Computational Prodrug  
564 Design Methodology for Liposome Formulability Enhancement of Small-Molecule APIs.  
565 *Molecular Pharmaceutics* **2023**, *20* (4), 2119-2127.
- 566 25. Sutherland, J. J.; Daly, T. M.; Liu, X.; Goldstein, K.; Johnston, J. A.; Ryan, T. P., Co-  
567 Prescription Trends in a Large Cohort of Subjects Predict Substantial Drug-Drug Interactions.  
568 *PLOS ONE* **2015**, *10* (3), e0118991.
- 569 26. Haša, J.; Hanuš, J.; Štěpánek, F., Magnetically Controlled Liposome Aggregates for  
570 On-Demand Release of Reactive Payloads. *ACS Applied Materials and Interfaces* **2018**, *10*  
571 (24), 20306-20314.
- 572 27. Balouch, M.; Šrejber, M.; Šoltys, M.; Janská, P.; Štěpánek, F.; Berka, K., In silico  
573 screening of drug candidates for thermoresponsive liposome formulations. *Molecular Systems*  
574 *Design Engineering* **2021**, *6* (5), 368-380.
- 575 28. Gupta, R.; Badhe, Y.; Rai, B.; Mitragotri, S., Molecular mechanism of the skin  
576 permeation enhancing effect of ethanol: a molecular dynamics study. *The Royal Society of*  
577 *Chemistry Advances* **2020**, *10* (21), 12234-12248.
- 578 29. Schroeter, A.; Eichner, A.; Mueller, J.; Neubert, R. H. H., Penetration Enhancers and  
579 Their Mechanism Studied on a Molecular Level. In *Percutaneous Penetration Enhancers*  
580 *Chemical Methods in Penetration Enhancement: Modification of the Stratum Corneum*,  
581 Dragicevic, N.; Maibach, H. I., Eds. Springer Berlin Heidelberg: Berlin, Heidelberg, 2015; pp  
582 29-37.
- 583 30. Amidon, G. L.; Lennernäs, H.; Shah, V. P.; Crison, J. R., A Theoretical Basis for a  
584 Biopharmaceutic Drug Classification: The Correlation of in Vitro Drug Product Dissolution  
585 and in Vivo Bioavailability. *Pharmaceutical Research* **1995**, *12* (3), 413-420.

- 586 31. Yalkowsky, S. H.; He, Y.; Jain, P., *Handbook of aqueous solubility data*. Chemical  
587 Rubber Company press: 2016.
- 588 32. O'Neil, M. J., *The Merck index: an encyclopedia of chemicals, drugs, and biologicals*.  
589 The Royal Society of Chemistry: 2013.
- 590 33. Pizzirusso, A.; De Nicola, A.; Sevink, G. J. A.; Correa, A.; Cascella, M.; Kawakatsu,  
591 T.; Rocco, M.; Zhao, Y.; Celino, M.; Milano, G., Biomembrane solubilization mechanism by  
592 Triton X-100: a computational study of the three stage model. *Physical Chemistry Chemical*  
593 *Physics* **2017**, *19* (44), 29780-29794.
- 594 34. Drabik, D.; Chodaczek, G.; Kraszewski, S.; Langner, M., Mechanical Properties  
595 Determination of DMPC, DPPC, DSPC, and HSPC Solid-Ordered Bilayers. *Langmuir* **2020**,  
596 *36* (14), 3826-3835.
- 597 35. Curtis, E. M.; Hall, C. K., Molecular Dynamics Simulations of DPPC Bilayers Using  
598 "LIME", a New Coarse-Grained Model. *The Journal of Physical Chemistry B* **2013**, *117* (17),  
599 5019-5030.

600

#### 601 **Acknowledgments**

602 F.Š. would like to acknowledge support by the Czech Science Foundation (project no. 19-  
603 26127X).

604

#### 605 **Conflict of interest statement**

606 The authors declare no conflict of interest, financial or otherwise.

607

#### 608 **Author contribution**

609 K.O. – Methodology development, experimental investigation, mathematical model  
610 development, data analysis, manuscript writing.

611 M.B. – Methodology development, experimental investigation, mathematical model  
612 development, data analysis, manuscript writing

613 K.S. – Permeability data analysis, manuscript writing

614 A.Z. – Instrumental analytical method development, liposome preparation, manuscript writing

615 K.B. – Supervision, results interpretation, manuscript writing

616 F.S. – Project idea conception, funding acquisition, supervision, results interpretation,  
617 manuscript writing